ELSEVIER

0955-2219(95)0006-2

Journal of the European Ceramic Society **15** (1995) 395–404
© 1995 Elsevier Science Limited
Printed in Great Britain. All rights reserved
0955-2219/95/$9.50

Reliability of Alumina Ceramics: Effect of Grain Size

Jürgen Seidel, Nils Claussen & Jürgen Rödel[a]

Advanced Ceramics Group, Technische Universität Hamburg-Harburg, Germany

(Received 16 February 1994; revised version received 20 September 1994; accepted 12 December 1994)

Abstract

The grain size dependence of fracture strength and Weibull modulus of alumina using a high purity, commercial starting powder was investigated. In the regime of an average grain size between 1·7 and 11 μm, fracture strength increases with decreasing grain size. This behaviour could be explained quantitatively by modelling the failure-causing defect as either a spherical pore or a hemispherical surface pit with a circumferential crack proportional to the average grain size. No dependence of Weibull modulus on average grain size and hence on R–*curve behaviour could be observed. Theoretical considerations show that the closure stresses in alumina responsible for the* R–*curve behaviour are too low to affect the Weibull modulus.*

1 Introduction

The reliability of ceramics is governed by two factors; the strength and the variability of strength. In developing a material for structural applications, for example a turbo charger for heat engines, a low probability of failure can be realized either by a high Weibull modulus and a moderate characteristic strength or by a high characteristic strength and a lower Weibull modulus.[1]

An approach to increase the strength of polycrystalline ceramics is afforded by the reduction of the average grain size.[2–7] The relationship between strength and grain size has generally been described using a σ versus $G^{-1/2}$ (strength versus inverse square root of the average grain size) diagram. With large grain sizes, an increase in strength with decreasing grain size is observed. In this regime (Orowan-branch) the average grain size is larger than the flaw size due to processing defects (pores, inclusions etc), so the strength determining defect scales with the average grain radius. In the fine grain size regime (Petch-branch) the size of the processing defects is larger than the grain size. In this region only a slight increase of strength[2–6] or even a constant strength level[7] have been observed with decreasing grain size. Due to the relevance of high strength for reliability, (sufficient strength levels could only be achieved in the fine grain size regime), it is of fundamental importance to understand the grain size dependence of flexure strength. Various interpretations of the transition between the two regimes and the failure mechanism at finer grain sizes have been proposed: crack initiation through microplasticity,[2,5] the dominance of processing flaws with a microstructural dependence attributable to a monocrystal to polycrystal increase in crack resistance[3] and the variation of fracture energy with grain size.[3,4] While the early debate was based on a single value toughness for a given grain size; (the influence of a rising *R*–curve on the strength), grain size behaviour has now also been considered.[6] Then the focus remained on the low strength Orowan-branch.[6]

The second feature concerning reliability is the variability of the strength values, generally expressed by the two parameter Weibull statistics.[8] Simple theoretical models lead to the postulate of an increased Weibull modulus if *R*–curve behaviour exists.[9–12] Steinbrech *et al.*[13] demonstrated that the toughness of a coarse grained, 16 μm alumina increases from about 3 MPa $m^{1/2}$ to 6 MPa $m^{1/2}$ over a crack extension of several mm. For alumina it is well appreciated that the plateau value of the *R*–curve increases with the average grain size, due to bridging interaction.[6,13,14]

Possible complications due to residual stresses related to machining damage are considered in a second paper.[15]

In the present study we focus on the grain size dependence of flexure strength in the fine grain

[a]Now at TH Darmstadt, Ceramics Group, FB Materialwissenschaft, GDP, Gebäude D, Hilperstraße 31, Darmstadt, Germany.
This work was supported by the Deutsche Forschungsgemeinschaft under contract number C1 53/13-2.

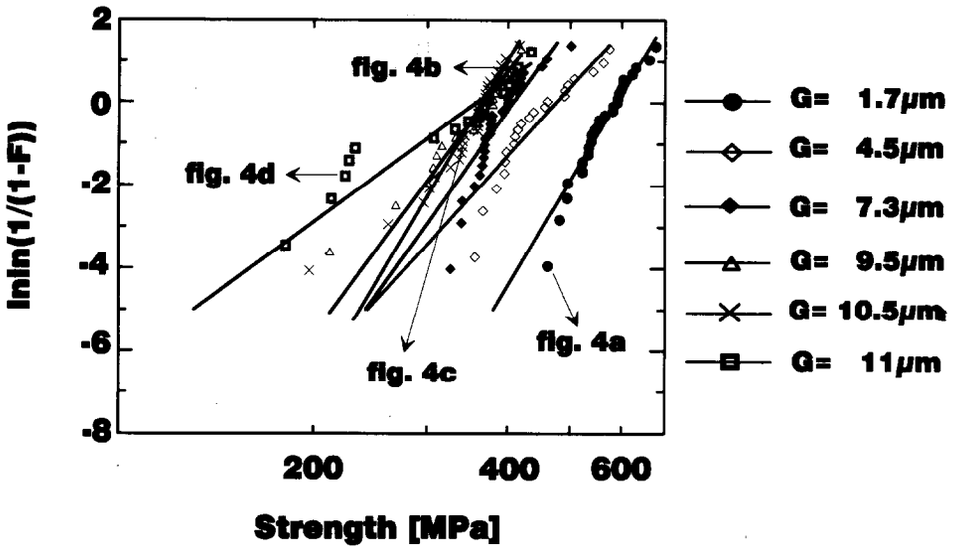

Fig. 1. Strength distributions (Weibull plot) of alumina materials with different grain size.

size regime and present new data, as well as a simple fracture mechanical model which allows rationalization of the observed experimental findings. The general knowledge of grain size dependent R–curve behaviour in alumina is further applied to discuss the influence of the R–curve behaviour on Weibull modulus m, again under application of a simple model to account for the experimental values. Specifically, the key question may be posed as: can the decreasing strength with increasing average grain size be compensated by an enhanced Weibull modulus due to an increasing crack resistance?

2 Experimental Procedure

A commercial, ultrafine Al_2O_3 powder (Taimei Chemical Co., Ltd, TM-DAR) was used to fabricate bars (4 × 5 × 40 mm) by uniaxial pressing the as received powder at 50 MPa in a steel die followed by cold isostatical pressing at 800 MPa. Green densities of 55% of the theoretical density were attained by this procedure. The green bars were sintered at temperatures of either 1350 or 1600°C in air. The lower sintering temperature was used to produce a fine grained material and the coarse grained materials were sintered at 1600°C at different dwell times (10 min to 96 h) to alter the average grain size. The sintered densities measured by the Archimedes method using water as immersion liquid were greater than 99% TD. After preparing the surfaces by grinding and polishing the microstructure was revealed by thermal etching for 30 min at temperatures 20°C below sintering temperature for the fine grained material and 50°C for the coarse grained materials. The average grain diameter were measured using the linear intercept technique. The average grain sizes could thus be adjusted in a regime between 1·7 and 11 μm. Prior to strength testing each bar was ground to 3 × 4 mm by a rotating diamond disk.

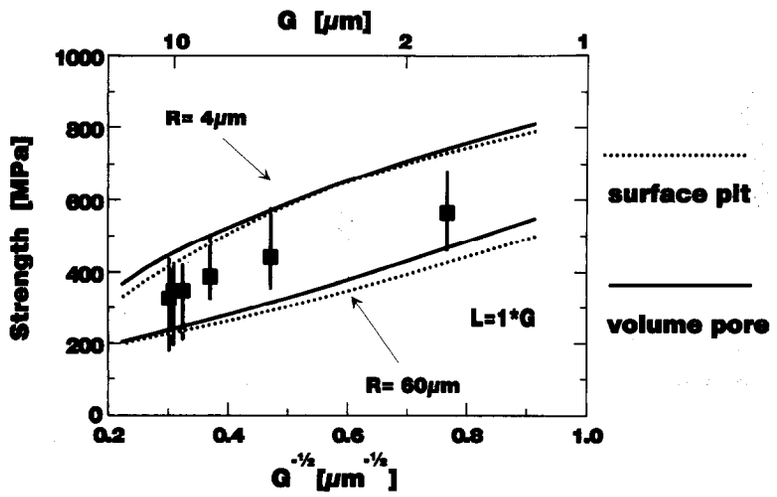

Fig. 2. Strength as function of the average grain size; solid lines represent the computed grain size dependence of strength assuming a spherical pore with an annular crack as fracture origin, dashed lines use the assumption of a hemispherical surface pit with a peripheral crack as a fracture origin.

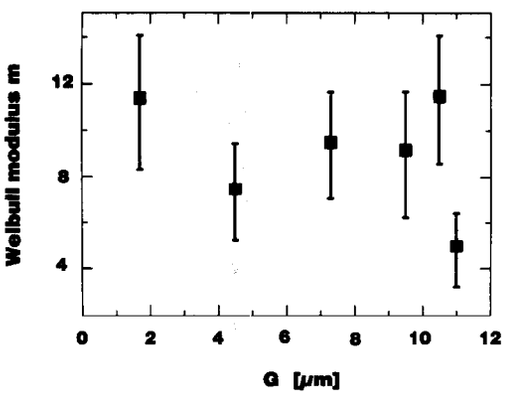

Fig. 3. Weibull modulus and 90%-confidence intervals as function of the average grain size.

The prospective tensile surfaces were finally ground with a 15 μm disk and polished by hand to a 3 μm finish. Uniaxial strength testing was carried out with a four-point bending test device, span lengths 10 and 20 mm with 20–30 bars for each batch in laboratory atmosphere of about 50% relative humidity. The loading rate was 1 mm/min.

The variability of the strength values was analysed corresponding to the 2 parameter Weibull approach, expressed by eqn 1 (with σ the fracture strength and σ_0 the Weibull scale parameter):

$$F = 1 - \exp(-(\frac{\sigma}{\sigma_0})m) \quad (1)$$

The strength values were ranked in ascending order and each strength value was associated with a fracture probability F evaluated by (with n the total number of specimens and i the i'th specimen):

$$F = \frac{i - 0{\cdot}5}{n} \quad (2)$$

The Weibull modulus, m and the 90% confidence intervals were evaluated using the maximum likelihood method.

Scanning electron microscopy was used to examine the fracture surfaces and to identify the strength determining defects.

3 Results

Figure 1 shows the strength distributions of the alumina batches with different grain size. The solid lines through the strength data are the curves representing the fit on the basis of the 2 parameter Weibull approach with the parameters m and σ_0.

Replotting the data as mean strength versus inverse square root of grain size shows the clear trend of an increasing strength with decreasing average grain size G (Fig. 2) with a rise of σ from 325 MPa at an average grain size of 11 μm to 564 MPa at G = 1·7 μm. Evaluation of the Weibull parameter m using the maximum likelihood method yields, with one exception, Weibull moduli ranging from 8 to 11 (Fig. 3). If the confidence intervals are included (Fig. 3) no dependence of m on G in the grain size region up to 11 μm could be observed. Not all the strength data correlate well with the corresponding Weibull parameter fit (Fig. 1). The small grain size materials exhibit a tendency to a low strength cut-off which may be better described by a three parameter Weibull approach, while the material with G = 11 μm might be better fitted by a bimodal strength distribution.

Most of the fracture surfaces investigated reveal volume defects in the form of large voids near the tensile surface as failure source (Fig. 4(a)–(c) see also Fig. 1). In a few cases surface flaws could be identified (Fig. 4(d) see also Fig. 1). There is no indication of a change of the defect character with grain size. Fig. 4(a)–(c) shows the fracture origins from specimens with three different grain sizes. The diameter of the defects (2R) in a batch with identical average grain size ranges from 20 to 80 μm. There is no indication for increasing defect sizes with increasing grain size.

4 Discussion

4.1 Strength as a function of grain size

Our experimental data confirm earlier experimental observations[2–6] of an increasing strength (as in our case by about 240 MPa) with decreasing grain size (in going from 11 to 1·7 μm). In the last decade this increase has been attributed to the increase of fracture toughness (or fracture energy) with grain size.[3,4] Fracture toughness, however, ought to be described by means of toughness as a function of crack length (R–curve), with the toughness at instability, as determined in a fracture test, being of particular interest. Steinbrech stated, that for strength considerations in alumina, the starting value of the R–curve — certainly more than the plateau value — is of special interest.[13,16] Therefore, most of the techniques to measure fracture toughness data are of little significance for strength issues. The starting value of the R–curve could be defined as the crack initiation toughness[13,16–18] as intrinsic,[19] or as crack tip toughness.[20] The term initiation toughness can be misleading, since it can be taken as a measure for a stress magnification before a notch or pore to initiate a crack rather than the stress intensity at the tip of an already existing crack required to define crack equilibrium. Experimental determination of the crack tip toughness is

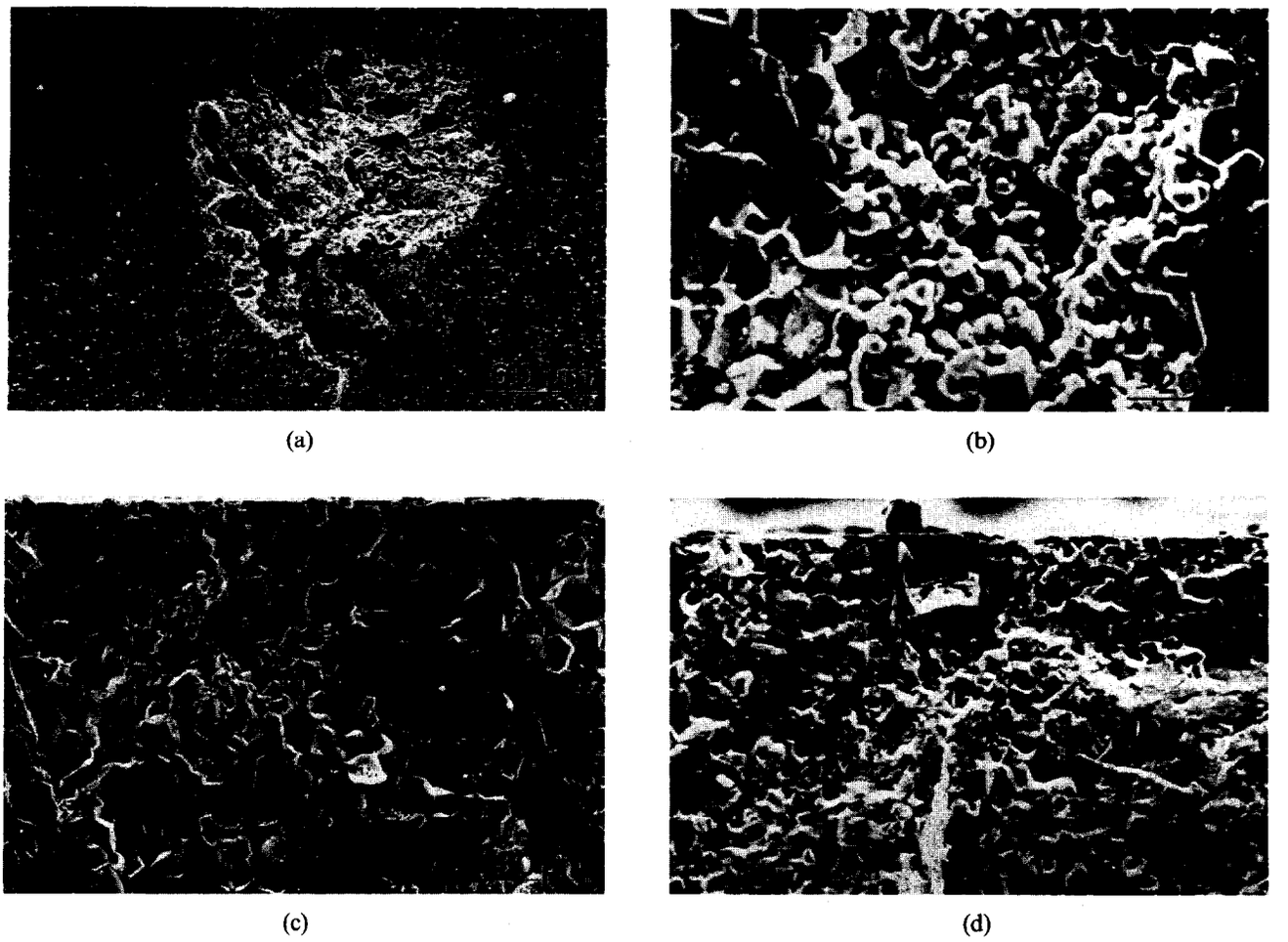

Fig. 4. Fracture surfaces of samples with different grain sizes; (a) G = 1·7 μm, σ = 461 MPa; (b) G = 11 μm, σ = 414 MPa; (c) G = 10·5 μm, σ = 340 MPa; (d) G = 11 μm, σ = 224 MPa; (a)–(c) Volume defects; (d) surface defects.

afforded by measuring the crack opening displacement (COD) near the crack tip.[20–22] This method has been applied to a hot pressed alumina of grain size 11 μm,[21] and a whisker — reinforced alumina.[22] Recently, the dependence of crack tip toughness on grain size in alumina has been investigated[20] and yielded no functional dependence, but an average crack tip toughness, K_0 = 2·3 MPa m$^{1/2}$ for all grain sizes investigated. The concept of a single valued toughness alone is therefore not sufficient to explain the observed dependence of strength on grain size.

Our alumina fractography points to pores (large voids) in the volume as major failure origin, with some occurrence of surface flaws also. Fractography also reveals that the pore size is independent of the grain size. This result can be predicted in applying the knowledge of the current sintering literature,[23] as long as no external pressure is applied and the sintering pressure is thereby only related to grain and pore curvature. In polycrystalline bodies pores should not cause fracture directly, because the stress concentration due to a pore is usually not sufficient to cause specimen fracture from the void surface. Evans and Davidge[24] as well as other authors[25,26] suggested that the pore of radius R is accompanied by a circumferential crack of length L (Fig. 5). The distance $R + L$ is taken as the initial crack length c_0, the crack length after a certain degree of stable crack growth is taken as c. Baratta,[27,28] Green[29]

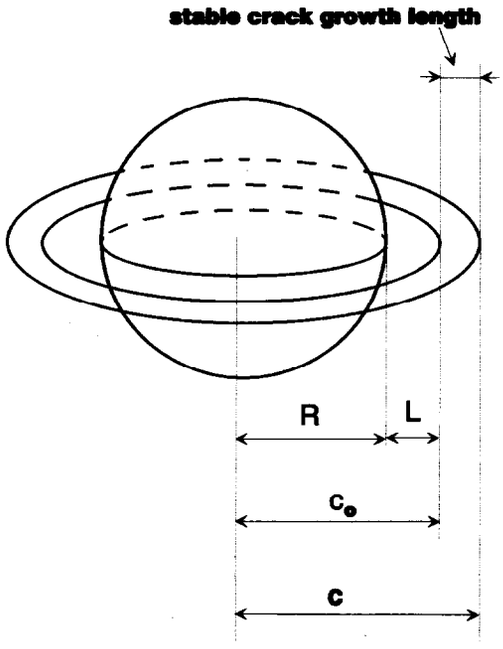

Fig. 5. Pore (void) with a circumferential crack (geometrical parameters).

and Fett[30] modelled this crack configuration and presented solutions for the normalized stress intensity factor in dependence of the ratio of L/R. On this basis it is possible to explain the grain size dependence of fracture strength assuming a pore with a circumferential crack as failure origin. For an evaluation it is assumed that the circumferential crack is proportional to the average grain size, whereas the pore sizes are constant. Equation 3 can then be used to calculate the grain size dependence of strength:

$$K_0 = \sigma \cdot \sqrt{\pi L} f(\frac{L}{R}) \quad (3)$$

The circumferential crack length is discussed in the literature to be a few grains in extent (one to three times the grain size) and perhaps vary with pore size.[3,10] In order to describe the grain size dependence of strength the exact length of the circumferential crack is of secondary nature. The basic assumptions are only that the circumferential crack length is proportional to the average grain size. Further to that, the toughness at instability is equal to the crack tip toughness, K_0. Since the stress in eqn 3 is the stress around the pore or surface pit, which in the first case is not exactly equal to the nominal flexure stress, a further small inaccuracy comes in. This is expected to be irrelevant since the volume flaws were close to the surface and thus differences in stress levels between pore location and surface were minute. To compute the grain size dependent strength for a defect modelled as a spherical pore/circumferential crack pair, we applied eqn 3 in the form given by Baratta[28] with the pore radii, R, then lying between 4 and 60 μm and the circumferential crack length $L = 1{\cdot}G$. To compare our results with possible surface defects as fracture origins, we also performed the equivalent calculation for the peripherally cracked hemispherical surface pit. For both computations, the tabulated values for $f(L/R)$ were utilized and an interpolation function used for the computations.

The solid lines in Fig. 2 show the result of the calculations for these two different pore sizes with the defect modelled as a volume flaw, while the dashed lines give the results for the hemispherical surface pit. The theoretical fits are very similar for both types of defects and in good agreement with the experimentally observed strength values, especially reflecting the decreasing strength with increasing grain size. Discrepancy between this model and the observed strength values can arise from the irregular shape of the pores in the alumina bodies. Uematsu *et al.*[26] measured the size and the size distribution of such irregularly shaped voids in hot isostatically pressed, translucent alumina. They found pore sizes up to 70–80 μm in radius, which is consistent with our calculations.

Although the assumption of a spherical pore or a hemispherical surface pit with a circumferential crack proportional to the average grain size is only an auxilliary means, it provides a plausible model to fit our experimental data. This simple model describes the grain size dependence of strength in both limiting cases, where the grain size is either larger or smaller than the initial flaw size, as well as the transition between the two.

Recently the model of a pore accompanied by a circumferential crack received further credibility by an acoustic emission investigation in alumina of various grain sizes.[31] It was found, that at a critical stress, which decreases with increasing grain size, acoustic events increased rapidly before failure. These events were located in the area where final failure occurred. One may therefore tentatively conclude, that an instability causing pore provides a stress magnification in the surrounding matrix sufficient to cause microcracking which occurs at a stress before final failure results. Physical reality may therefore be a pore with distributed microcracking at its perimeter, which is here modelled with a continuous circumferential crack. However, the actual existence of circumferential cracks around pores, be they complete or incomplete, still needs to be verified.

4.2 Weibull modulus as a function of grain size

The second feature concerning reliability is the variability of strength, normally expressed by the Weibull modulus m. The present study has shown that the Weibull modulus does not change in the grain size regime from 1·7 to 10·5 μm. The alumina of the largest grain size G = 11 μm) exhibited the smallest Weibull modulus with m = 5·8. Here the possibility of localized abnormal grain growth, which introduces a second flaw population, might already come into play. In the literature, systematic studies in the same material on the grain size dependence of the Weibull modulus are rare. Scholten *et al.*[32] for example investigated two different aluminas, a commercially available powder with an average grain size (after sintering) of 50 μm and a laboratory scale alumina with 10 μm. For the uniaxial, four-point bend test, the Weibull modulus for these two different materials was 21·6 and 6·7, respectively. In this context Scholten *et al.* denied the influence of the R–curve to explain the great difference in strength variability. For alumina, a Weibull modulus $m > 20$ has also been reported by Miyashita *et al.*[33] who demonstrated the influence of the compaction pressure on the Weibull modulus. They reported an increasing Weibull modulus with decreasing compaction

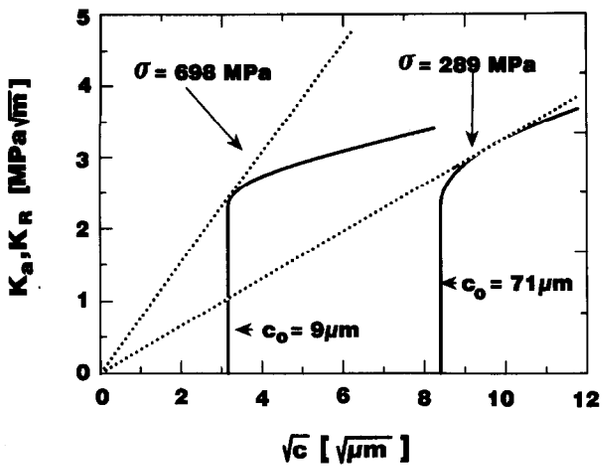

Fig. 6. *R*–curves and instability criterion for different initial flaw sizes (crack is modelled as a penny crack).

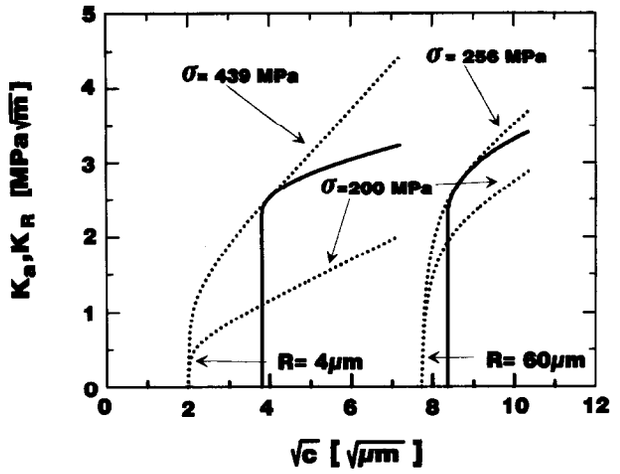

Fig. 7. *R*–curves and instability criterion for different pore sizes for the low strength material (crack configuration: pore + annular crack).

pressure, with a concurrent decrease in strength. Again, it should be emphasized that for reliability both a high strength as well as a high Weibull modulus is aspired. The Weibull moduli reported from other authors[34–36] range between 8 and 13. The important result of this study is that the disadvantage of decreasing strength with increasing grain size could not be compensated by the advantage of an increasing Weibull modulus. The higher plateau toughness of coarse grained, as compared to fine grained alumina, has no influence on the Weibull modulus. In the following section we discuss this result in greater detail.

Long crack *R*–curves of alumina ceramics have been determined by various groups.[13,16,37] In the last few years, efforts were made to measure the *R*–curves from either natural short cracks or radial indentation cracks.[14,38,39] Due to the difficulty of measuring *R*–curves of cracks originating from pores (with the notable exception of Ce–TZP composites)[40] we tried to model the *R*–curve based on the fundamental description of closure stresses. These closure stresses arise from bridging interactions and result in a bridging term R_μ which has to be added to the starting value R_0 of the *R*–curve. For our considerations we resorted to a continuum concept with smoothly varying, delocalized closure stresses (an assumption, which needs to be qualified at a later time). The total crack resistance[19] can then be expressed by eqn 4 (with $p(u)$ the crack closure stress, p as a function of half of the crack opening, u):

$$R(c) = R_0 + R_\mu = R_0 + 2\int_0^{u_b} p(u)\mathrm{d}u \qquad (4)$$

If the COD ($2u$) reaches the value $2u_b$, the closure stresses have diminished to zero and hence the *R*–curve has reached the plateau toughness.

In order to express this relationship in terms of stress intensity factors, R_0 and R_μ[19] can be transformed into K_0 and K_μ by eqns 5 and 6 (E is Young's modulus):

$$K_0 = \sqrt{R_0 \cdot E} \qquad (5)$$

$$K_\mu = \sqrt{K_0^2 + E \cdot R_\mu} - K_0 \qquad (5)$$

In the following calculation we considered the influence of closure stress on the Weibull modulus and on characteristic strength. We used two complementary approaches: Firstly, we modelled the crack as a penny-shaped crack of initial length c_0 (Fig. 6). Secondly, we applied the pore/annular crack configuration as introduced before (Fig. 7).

For mathematical simplicity we started to model the crack configuration pore with an annular crack as a penny crack. When the crack extended stably the closure stresses were only effective between c_0 and c (Fig. 5). Using the weight function of the penny crack geometry the *R*–curve ($K_R(c)$) is described by eqn 7 (where the closure stresses are taken as a function of r only):

$$K_R(c) = K_0 + \int_{c_0}^{c} p(r)\,\frac{r}{\sqrt{c^2 - r^2}}\,\mathrm{d}r \qquad (4)$$

In the very small regime of possible stable crack growth the closure stresses were taken as constant (Dugdale zone), and assumed to be equal to the peak closure stress, p_m (which occurs near the crack tip in alumina).[21]

In order to examine whether the closure stresses cause a deviation from linear behaviour in the Weibull plot we do not resort to the measured strength distributions, since some distributions deviate from exact linear behaviour due to different failure origins. For further calculations we assumed a strength distribution with the Weibull parameter m = 10 and σ_0 = 589 and 365 MPa, similar to the measured distributions with an average grain size of 1·7 and 10·5 μm, respectively,

but without any *R*–curve. Equation 8 was used to transform the strength distribution into a flaw size distribution, providing the initial crack length c_0, whereby a single valued crack tip toughness K_0 = 2·3 MPa $m^{-1/2}$ (independent of grain size) was assumed:[20]

$$K_0 = \frac{2}{\sqrt{\pi}} \cdot \sigma \cdot \sqrt{c_0} \tag{8}$$

The next step is to attach the *R*–curves to the initial crack length c_0. This is demonstrated in Fig. 6. The instability criterion, eqns 9 and 10,

$$K_a = K_R(c) \tag{9}$$

$$\frac{dK_a}{d_c} = \frac{dK_R(c)}{d_c} \tag{10}$$

was taken to calculate the crack length at instability as well as the corresponding strength. This is also shown schematically in Fig. 6.

The calculation was carried out for two peak closure stresses of p_m equal to either 40 or 120 MPa, the upper and lower bounds reported in the literature.[21,41,42] The degree of stable crack growth is found to increase with decreasing strength and increasing closure stress. The stable crack growth length and accordingly the toughness at instability increases with c_0 (Fig. 6). The computation yields a stable crack growth length of 0.5 μm for an initial crack length of 9 μm with a strength increase from 678 to 698 MPa at a K_{Ic} of 2·44 MPa $m^{1/2}$. For a specimen with a large initial flaw size, e.g. c_0 = 71 μm, σ = 243 MPa (without *R*–curve) the stable crack growth length is predicted to be 22·6 μm with instability occurring at 289 MPa at 3·15 MPa $m^{1/2}$. Therefore strength increase due to *R*–curve behaviour is more pronounced for a lower initial strength and hence an increasing

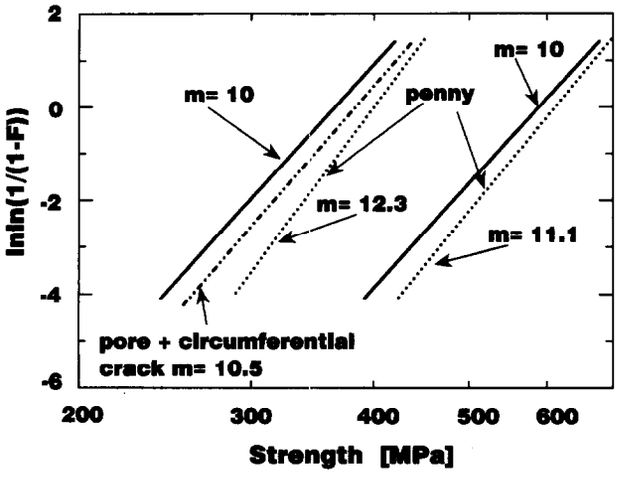

Fig. 8. Influence of constant closure stress of 120 MPa on the strength distributions of material characterized by m = 10 and σ_0 = 365 MPa and 589 MPa, respectively, assuming a penny crack geometry or a pore with an annular crack.

Weibull modulus should be the result. In Fig. 8 the influence of the closure stress of 120 MPa on Weibull modulus and characteristic strength is described. The two initial distributions are shifted to higher strength and the Weibull modulus increases from m = 10 to m = 12·3 for the low strength material and to m = 11·1 for the high strength material. Again, the effect of the closure stress is more evident at lower strength. Still, the increase of the Weibull modulus due to the closure stress of 120 MPa is relatively small. If we carry out the same calculation for a closure stress of 40 MPa the increase in σ_0 and m is negligible. For the high and the low strength material the increase of the characteristic strength is lower than 5 MPa and the Weibull modulus increases from 10 to 10·5. This calculated change would be statistically insignificant in practice for typically 20–30 test pieces. For all computations with the parameter sets used here, the closure stresses do not cause a deviation from linear behaviour in the Weibull plot.

In the calculation presented above the crack configuration was modelled as a penny crack with no bridging interactions at the initially existing crack faces. Different strength values had to be obtained by using different lengths of starting cracks, c_0. In the following section we compute the variation of strength and Weibull modulus for the crack configuration of a pore with a circumferential crack and thereby relate back to the model which could account for grain size dependent strength introduced in the earlier chapter. Again we assume strength distributions with the Weibull parameter m = 10 and σ_0 = 365 MPa (G = 10·5 μm) and σ_0 = 589 MPa (G = 1·7 μm), respectively. For the described crack configuration Barattas solution[28] (eqn (3)) for the stress intensity factor was used to evaluate the pore sizes assuming $L = G$ for the initial circumferential crack length using K_0 = 2·3 MPa $m^{1/2}$. The *R*–curves (eqn (11)) were calculated using a weight function proposed by Fett.[30] It is assumed that the *R*–curves start at $R + 1{\cdot}G$:

$$T(c) = K_0 + p_m \beta \sqrt{\frac{2}{\pi L}} \int_G^L \left(\frac{1}{\sqrt{1-\frac{r}{L}}} + 0{\cdot}6147\sqrt{1-\frac{r}{L}} + 0{\cdot}2502\sqrt{\left(1-\frac{r}{L}\right)^3} \right) dr + \frac{2p_m(1-\beta)}{\sqrt{\pi(L+R)}} \int_G^L \frac{r+R}{(L+R)^2-(r+R)^2}\, dr \tag{11}$$

with β defined by

$$\beta = \frac{1}{(1+2\cdot\frac{L}{R})^2} \tag{12}$$

The instability criterion (eqns 9 and 10) was used to calculate the degree of stable crack growth prior to failure and the corresponding strength. In Fig. 7 the R–curve and the tangency points are sketched for the low strength material for two different pore sizes. The circumferential crack length increases from $L = G = 10{\cdot}5$ μm (starting point of the R–curve) to $L = 15{\cdot}4$ μm at instability ($p_m = 120$ MPa, $R = 60$ μm) with $K_{Ic} = 2{\cdot}73$ MPa $m^{1/2}$ and an increase in strength due to crack bridging from 243 to 256 MPa. The computation for a specimen with small initial pore size ($R = 4$ μm) yields a stable crack growth regime of $1{\cdot}4$ μm and a strength increase from 420 to 439 MPa with instability occurring at 2·52 MPa $m^{1/2}$.

The influence of closure stresses of 120 MPa on the characteristic strength and the Weibull modulus of the low strength material is shown in Fig. 8. σ_0 increases from 365 to 383 MPa and the Weibull modulus from 10 to 10·5. As mentioned above the strength distribution of the high strength material remains unaffected. At a closure stress of 40 MPa the strength distributions of both materials were essentially not influenced.

In summary, the calculation for the crack configuration pore with circumferential crack yields a smaller influence of the closure stresses on the mechanical properties compared to the case when the pore is modelled as a penny crack. This trend may be appreciated if the greater stress concentration at larger pore sizes — in the pore/annular crack model — is taken into account. This results in a stronger increase of K_a with the applied stress σ at larger pore sizes. For the same externally applied stress σ (for example in Fig. 7, $\sigma = 200$ MPa) and the same annular crack length L, K_a is larger at larger pore sizes. Therefore the higher degree of stable crack growth at larger pore sizes associated with a higher crack resistance and with a stronger increase of the initial strength is compensated by a stronger increase of K_a with σ at larger pore sizes. All subleties aside, however, both models are able to reproduce the experimental findings very well and only predict small differences in the increase in Weibull modulus with incorporated R–curve.

The calculations have shown that even at relatively high closure stresses (120 MPa), only a small increase of the Weibull modulus could be achieved, which is consistent with our experimental data. Three qualifications in using our modelling approach should be considered at this point.

Firstly, in assuming a Dugdale zone, we did not specify u_b in eqn 4. Since the instability criteria was met in all computations at very low toughness values ($K_{Ic} < 3{\cdot}2$ MPa $m^{1/2}$), well below commonly reported toughness values for alumina, the plateau value of the R–curve as well as the exact position of the last active bridge are irrelevant in strength considerations of alumina ceramics. Specifically, it is evident, that the long crack toughness values measured in crack bridging materials are not pertinent for strength issues (except for very short, steep R–curves).

Secondly, the computations are strictly relevant only for a continuum with delocalized closure stresses. This condition is not met for grain bridging materials with grain sizes at the order or even larger than our calculated stable crack growth lengths. Since the distribution of bridges in the matrix is unknown, an inclusion of grain-localized stresses in the model, however, would be rather arbitrary. The current model, therefore, serves as the best possible indication for the actual occurring stable crack growth as well as the K_{Ic} values applicable for fracture testing.

Thirdly, the second model of a pore with a circumferential crack hinges critically on the very existence of microcracking around a pore. Indications for the physical reality of this model, however, have been provided recently.[31] This concept can also be understood as a strategy to design high strength materials. These may be manufactured, if microcracking around failure causing pores can be suppressed.

Our results point to the relevance of the ratio of closure stress to failure stress. In material development efforts, both material characteristics need to be appreciated. If microstructural design initially focuses on preparing a relatively weak, but flaw tolerant material, then an increase of strength will not necessarily yield a strong, flaw tolerant material, since the ratio of closure stress to fracture strength decreases. On the other hand, if the effect of closure stress on strength and strength variability is to be considered and even utilized as a measurement tool to compute the closure stresses, a low strength material ought to be employed. This approach was indeed taken by Fett and Munz,[42] who demonstrated a deviation from linear behaviour in the Weibull plot for a low strength, coarse grained alumina. This deviation is only relevant at low strength (about 200 MPa) and is attributed to the R–curve behaviour. This observation supports the result of the present investigation that the closure stresses in alumina do only affect the variability of strength at a very low strength level.

The question posed in the introduction can now be answered: for alumina ceramics a small grain size and therefore high average strength has to be favoured compared to a large grain sized alumina with low average strength, albeit long crack R–curve behaviour. This result is independent of the specific flaw type and specifically holds both

for penny shaped cracks as well as for pores with circumferential cracks. Only in applications where excessive damage may occur[6] and low strengths are tolerable, a large grain sized alumina ought to be chosen as a load bearing material.

Conclusions

(1) The strength in alumina increases with decreasing average grain size from 564 MPa at 1·7 μm to 320 MPa at 11 μm.
(2) This grain size dependence of strength can quantitatively be described by models based on either a spherical pore/circumferential crack combination or a hemispherical surface pit/peripheral crack combination.
(3) Weibull modulus m showed no dependence on grain size.
(4) A simple Dugdale zone model attached to a distribution of flaw sizes can explain the invariability of the Weibull modulus on grain size and R–curve behaviour and points to the importance of the peak closure stress, which, according to literature values appears too low to affect the Weibull modulus of alumina significantly.

Acknowledgements

The authors wish to thank Dr T. Fett for supplying his results concerning the weight function of a void with an annular crack prior to publication, Prof. R. Bordia is thanked for helpful discussions. The reviewers comments are also appreciated for being very helpful.

References

1. Musicant, S., *What every engineer should know about ceramics*. Marcel Dekker, Inc. 1991.
2. Rice, R. W., Strength grain size effects in ceramics. *Proc. Brit. Ceram. Soc.*, **20** (1972) 205–7.
3. Rice, R. W., Microstructure dependence of mechanical behaviour. In *Treatise on materials science and technology.*, Vol. 11, ed. R. K. MacCrone. 1977, pp. 199–381.
4. Dörre, E. & Hübner, H., *Alumina Processing, Properties and applications*. Springer Verlag, New York, 1993.
5. Carniglia, S. C., Reexamination of experimental strength-vs-grain-size data for ceramics. *J. Am. Ceram. Soc.*, **55** (1972) 243–9.
6. Chantikul, P., Bennison, S. J. & Lawn, B. R., Role of grain size in the strength and R–curve properties of alumina. *J. Am. Ceram. Soc.*, **73** (1990) 2419–27.
7. Alford, N. M., Kendall, K., Clegg, W. J. & Birchall, J. D., Strength/microstructure relation in Al_2O_3 and TiO_2. *Advanced Ceramic Materials*, **3**, (1988) 113–7.
8. Weibull, W., A statistical distribution function of wide applicability. *J. Appl. Mech.*, **18** (1951) 293–7.
9. Cook, R. F. & Clarke, D. R., Fracture stability, R–curves and strength variability. *Acta Metall.*, **36** (1988) 555–62.
10. Shetty, D. K. & Wang, Jr, S., Crack stability and strength distribution of ceramics that exhibit rising crack-growth-resistance (R–curve) behavior. *J. Am. Ceram. Soc.*, **72** (1989) 1158–62.
11. Bennison, S. J. & Lawn, B. R., Flaw tolerance in ceramics with rising crack resistance characteristics. *J. Mat. Sci.*, **24** (1989) 3169–75.
12. Tandon, R., Green, D. J. & Cook, R. F., Strength variability in brittle materials with stabilizing and destabilizing resistance fields. *Acta Metall. Mater.*, **41** (1993) 399–408.
13. Steinbrech, R. W., Reichl, A. & Schaarwächter, W., R–curve behavior of long cracks in alumina. *J. Am. Ceram. Soc.*, **73** (1990) 2009–15.
14. Braun, L. M., Bennison, S. J. & Lawn B. R., Objective evaluation of short-crack toughness curves using indentation flaws: case study on alumina-based ceramics. *J. Am. Ceram. Soc.*, **75** (1992) 3049–57.
15. Seidel, J., Claussen, N. & Rödel, J., Reliability of alumina: II. Effect of processing technique and testing procedure. To be submitted to *J. Eur. Ceram. Soc.*
16. Steinbrech, R., Knehans, R. & Schaarwächter, W., Increase of crack resistance during slow crack growth in Al_2O_3 bend specimens. *J. Mat. Sci.*, **18** (1983) 265–70.
17. Mussler, B., Swain, M. V. & Claussen, N., Dependence of fracture toughness of alumina on grain size and test technique. *J. Am. Ceram. Soc.*, **65** (1982) 566–72.
18. Claussen, N., Mussler, B. & Swain, M. V., Grain-size dependence of fracture energy in ceramics. *J. Am. Ceram. Soc.*, **65** (1982) C14–6.
19. Lawn, B., *Fracture of brittle solids*. Cambridge University Press, 1993.
20. Seidel, J. & Rödel, J., Measurement of crack tip toughness in alumina as a function of grain size. To be published in *J. Am. Ceram. Soc.*
21. Rödel, J., Kelly, J. F. & Lawn, B. R., In-situ measurements of bridged crack interfaces in the scanning electron microscope. *J. Am. Ceram. Soc.*, **73** (1990) 3313–8.
22. Rödel, J., Fuller, Jr, E. & Lawn, B. R. In-situ observations of toughening processes in alumina reinforced with silicon carbide whiskers. *J. Am. Ceram. Soc.*, **74** (1991) 3154–7.
23. Slamovich, E. B. & Lange, F. F., Densification of large pores: II. Driving potentials and kinetics. *J. Am. Ceram. Soc.*, **76** (1993) 1584–90.
24. Evans, A. G. & Davidge, R. W., The strength and fracture of stochiometric polycristalline UO_2. *J. Nucl. Mater.*, **5** (1970) 314–25.
25. Rice, R. W., Pores as fracture origins in ceramics. *J. Mat. Sci.*, **19** (1984) 895–914.
26. Uematsu, K., Sekiguchi, M., Kim, J-Y., Saito, K., Mutoh, Y. Inoue, M., Fugino, Y., & Miyamoto, A., Effect of processing conditions on the characteristics of pores in hot isostatically pressed alumina, *J. Mat. Sci.*, **28** (1993) 1788–1992.
27. Baratta, F. I., Stress intensity factor estimates for a peripherally cracked spherical void and a hemispherical surface pit., *J. Am. Ceram. Soc.*, **61** (1978) 490–3.
28. Baratta, F. I., Refinement of stress intensity factor estimates for a peripherally cracked spherical void and a hemispherical surface pit., *J. Am. Ceram. Soc.*, **64** (1981) C3–4.
29. Green, D. J., Stress intensity factor estimates for annular cracks at spherical voids. *J. Am. Ceram. Soc.*, **63**, (1980) 342–4.
30. Fett, T., Stress intensity factors and weight function for a void with an annular crack. To be submitted to *Int. J. of Fract.*
31. Wakayama, S. & Kawahara, M., Evaluation of critical stress of microcracking in alumina. In *Austceram, Proc. of the Int. Conf. on Ceramics*, ed. M. J. Bannister, 1992, pp. 938–43.
32. Miyashita, M., Kim, J.-Y., Kata, Z., Uchida, N. & Uematsu, K., Effect of compaction pressure on the internal structure of sintered alumina. *J. Ceram. Soc. Jap. Int. Ed.*, **100** (1992) 1337–40.

33. Scholten, H., Dortmans, L., De With, G., Weakest-link failure prediction for ceramics: design and analysis of uniaxial and biaxial bend tests II. *J. Eur. Ceram. Soc.*, **10** (1992) 33–40.
34. Quinn, G., Flexure strength of advanced structural ceramics: A Round Robin, *J. Am. Ceram. Soc.*, **73** (1990) 2374–84.
35. Steen, M., Sinnema, S. & Bressers, J., Statistical analysis of bend strength data according to different evaluation methods. *J. Eur. Ceram, Soc.*, **9** (1992) 437–45.
36. Mosser, B. D., Reed, J. S. & Varner, J. R., Strength and Weibull modulus of sintered compacts of spray dried granules. *Am. Ceram. Soc. Bul.*, **71** (1992) 105–9.
37. Fett, T. & Munz, D., Evaluation of *R*-curve effects in ceramics. *J. Mat. Sci.*, **28** (1993) 742–52.
38. Steinbrech, R. W. & Schmenkel, O., Crack-Resistance Curves of Surface Cracks in Alumina. *J. Am. Ceram. Soc.*, **71** (1988) C271–3.
39. Krause, Jr, R. F., Rising fracture toughness from the bending strength of indented alumina beams. *J. Am. Ceram. Soc.*, **71** (1988) 383–43.
40. Ramachandran, N., Chao, L.-Y. & Shetty, D. K., *R*-curve behavior and flaw insensitivity of Ce–TZP/Al_2O_3 composite. *J. Am. Ceram. Soc.* **76** (1993) 961–8.
41. Fett, T. & Munz, D., Influence of bridging interactions on the lifetime behaviour of coarse-grained Al_2O_3. *J. Eur. Ceram. Soc.*, **12** (1993) 131–8.
42. Fett, T. & Munz, D., Estimation of bridging interactions for natural cracks from bending strength of coarse-grained Al_2O_3. Submitted to *J. Am. Ceram. Soc.*